Journal of Cosmology and Astroparticle Physics
An IOP and SISSA journal

Dark forces in the sky: signals from Z' and the dark Higgs

Nicole F. Bell, Yi Cai and Rebecca K. Leane

ARC Centre of Excellence for Particle Physics at the Terascale, School of Physics,
The University of Melbourne,
Victoria 3010, Australia

E-mail: n.bell@unimelb.edu.au, yi.cai@unimelb.edu.au,
rleane@physics.unimelb.edu.au

Received June 7, 2016
Accepted July 26, 2016
Published August 1, 2016

Abstract. We consider the indirect detection signals for a self-consistent hidden U(1) model containing a Majorana dark matter candidate, χ, a dark gauge boson, Z', and a dark Higgs, s. Compared with a model containing only a dark matter candidate and Z' mediator, the addition of the scalar provides a mass generation mechanism for the dark sector particles and is required in order to avoid unitarity violation at high energies. We find that the inclusion of the two mediators opens up a new two-body s-wave annihilation channel, $\chi\chi \to sZ'$. This new process, which is missed in the usual single-mediator simplified model approach, can be the dominant annihilation channel. This provides rich phenomenology for indirect detection searches, allows indirect searches to explore regions of parameter space not accessible with other commonly considered s-wave annihilation processes, and enables both the Z' and scalar couplings to be probed. We examine the phenomenology of the sector with a focus on this new process, and determine the limits on the model parameter space from Fermi data on dwarf spheriodal galaxies and other relevant experiments.

Keywords: dark matter theory, dark matter experiments

ArXiv ePrint: 1605.09382

doi:10.1088/1475-7516/2016/08/001

JCAP08(2016)001

Contents

1 Introduction **1**

2 Model setup **3**

3 Dark matter annihilation processes for indirect detection **5**
3.1 Annihilation cross sections 5
3.2 Decay widths of the dark Higgs and Z' 7

4 γ-ray energy spectra **8**

5 Annihilation limits from dwarf spheriodal galaxies and AMS-02 **9**

6 Other model constraints **11**
6.1 Collider and direct detection constraints 11
6.2 BBN and CMB constraints 12
6.3 Unitarity 12

7 Summary **12**

JCAP08(2016)001

1 Introduction

While dark matter (DM) is thought to be the dominant form of matter in the universe, its fundamental nature remains unknown. Of the many possible types of DM candidates, a particularly well motivated choice are Weakly Interacting Massive Particles (WIMPs) [1, 2]. This class of DM contains an abundance of models. In order to discover which of the many models may be the correct description, it is necessary to make contact between these theories and experiments. To efficiently test many of these models, it is desirable to investigate the properties of DM in a model independent manner wherever possible. This is reasonably achieved within the simplified model framework [3–10], where only the lightest particles in the theory are retained, and they can be generically explored via phenomenologically distinct couplings and mediator choices. Specifically, the three benchmark simplified models for DM and Standard Model (SM) interactions are a spin-1 mediated s-channel interaction, a spin-0 mediated s-channel interaction, and a spin-0 mediated t-channel interaction [8].

However, due to their simplified nature and reduced number of parameters, these benchmark models are not intrinsically capable of capturing the full phenomenology of many realistic UV complete theories. Perhaps worse is that the separate consideration of these benchmarks can lead to physical problems and inconsistencies. For instance, the consequences of gauge invariance and unitarity violation have recently been discussed in [11–25].

These issues motivate a scenario in which the vector and the scalar mediators appear together within the same theory.[1] Specifically, a simplified model with a spin-1 mediator and axial-vector couplings to fermions will lead to unitarity violation at high energies unless some additional new physics, such a scalar degree of freedom, is introduced to the simplified model setup [21]. This scalar is exceedingly well motivated if it is also taken to provide

[1] Some recent work on multi-mediator models can be found in refs. [26–29].

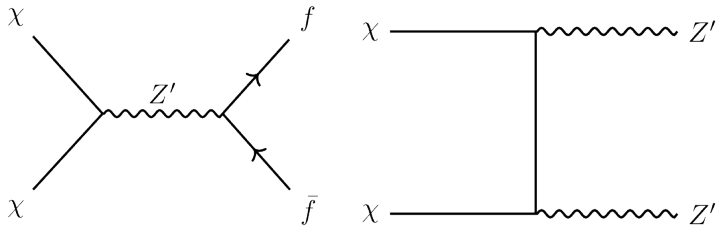

Figure 1. Spin-1 simplified model annihilation processes. Left: this process has an s-wave component only if the mediator has axial-vector couplings to SM fermions, f. However, the non-observation of a direct detection or LHC signal makes it difficult to obtain a thermal relic scale cross section from this diagram. Right: this process is s-wave for all field or coupling types and, as it can avoid LHC and direct detection bounds in the hidden on-shell mediator scenario, is often considered in the indirect detection context.

a mass generation mechanism for the dark sector, as the "dark Higgs". The purpose of this paper is to explore the indirect detection signals for a gauge invariant model where the dark sector consists of a fermionic DM candidate, a spin-1 mediator, and a dark Higgs field. In doing so, we shall encounter important phenomenology that cannot be captured by a single-mediator model.

In the indirect detection context, simplified models have commonly been used to investigate annihilation processes and place limits on the dark matter parameter space. Only annihilations which proceed via an s-wave process contribute substantially to DM signals in the universe today, as p-wave contributions are highly suppressed by a velocity squared factor, $v_\chi^2 \approx 10^{-6}$. Within the simplified model framework, spin-1 mediators provide two possible two-body s-wave annihilation processes for fermionic dark matter, as shown in figure 1. (i) $\chi\chi \to ff$ has an s-wave component provided the mediator has axial-vector couplings to SM fermions, f while (ii) $\chi\chi \to Z'Z'$ has an s-wave component for any (vector or axial-vector) coupling of the Z' to χ. The latter process, with the Z' pair produced on-shell, is commonly studied in the indirect detection context; it is capable of producing large annihilation signals while avoiding strong constraints imposed by collider and direct detection searches [30–34].

For spin-0 mediators, $\chi\chi \to ff$ is s-wave if the mediator is a pseudoscalar, but the couplings to SM fermions are strongly constrained, such that a thermal relic cross section is not easily obtained, nor a large indirect detection signal. The remaining 2-body annihilation processes for spin-0 mediators are all p-wave, meaning that to obtain a non-negligble indirect detection signal with non-excluded parameters, one needs to resort to the case where three spin-1 fields, s, are produced[2] as $\chi\chi \to sss$. While this is an s-wave process provided that the mediator is a pseudoscalar, it suffers from three-body phase space suppression [31]. These processes are shown in figure 2.

In this paper, we will show that once the dark Higgs is added to the dark sector, the indirect detection phenomenology considered previously was incomplete. Of particular interest will be the new s-wave annihilation process,

$$\chi\chi \to sZ'. \tag{1.1}$$

This is always an s-wave process, irrespective of whether the DM-Z' coupling is vector or axial-vector, and irrespective of whether s is a scalar or pseudoscalar. This process allows for

[2]A two-body s-wave process is possible for combinations of multiple distinct scalars [31, 32, 35], but this extends beyond the simplified model framework and requires more detailed model building.

JCAP08(2016)001

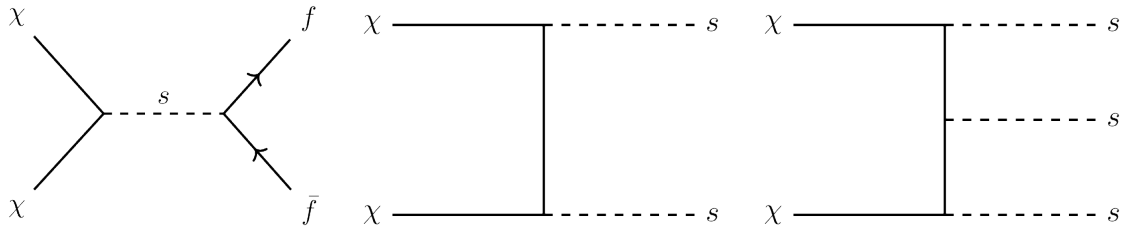

Figure 2. Spin-0 simplified model annihilation processes. Left: this process has an s-wave component if the spin-0 field is a pseudoscalar. However, the non-observation of a direct detection or LHC signal makes it difficult to achieve a thermal relic density with this process. Middle: this process is p-wave for all field or coupling types. Right: this process has an s-wave contribution if the spin-0 field is a pseudoscalar, but it is three-body phase space suppressed. There is no s-wave process for fermionic DM annihilation to a spin-0 field with scalar couplings.

JCAP08(2016)001

new, rich phenomenology. It allows the spin-0 particle to play an important role in indirect detection, which is not possible in models with only a spin-0 mediator due to the velocity or phase space suppressions of the annihilation diagrams in the pseudoscalar mediator case, and the complete absence of any s-wave annihilation processes in the scalar mediator case. Importantly, although both the $\chi\chi \to sZ'$ and $\chi\chi \to Z'Z'$ annihilation channels have an s-wave component, the sZ' channel tends to dominate when it is kinematically accessible. Neglecting this important annihilation process would lead to dramatically different results.

Hidden sector models [30–34, 36–58] are a specific realization of simplified models, commonly adopted in the indirect detection scenario because their small direct couplings to the SM ameliorate the tension between strong constraints from collider and direct detection experiments, and the goal of a sizeable indirect detection signal. If the DM annihilates to on-shell mediators (rather than directly to SM particles via off-shell mediators) the smallness of the dark-SM couplings are irrelevant for indirect detection, provided of course that the dark-sector mediators eventually decay to visible sector particles with lifetime shorter than the age of the galaxy. The signal size for indirect detection is instead set by the size of the dark sector couplings, which can often be taken to be quite large.

In this paper, we will investigate the phenomenology of these indirect detection signals for a self-consistent hidden U(1) sector, with a focus on the impact of this new $\chi\chi \to sZ'$ annihilation channel. In section 2, we will describe the model in detail. We will then list all the annihilation processes of interest in this model, along with the relevant cross sections and decay widths, in section 3. In section 4, we will simulate the consequent γ-ray spectra, which we will use in section 5 to calculate the limits on the cross section and parameter space from Fermi-LAT data on dwarf spheriodal galaxies, the most dark matter dense objects in our sky, as well as AMS-02. Finally we will consider relevant limits from unitarity and other experiments in section 6, and summarize in section 7.

2 Model setup

The gauge symmetry group for our model is $\mathrm{SU}(3)_c \otimes \mathrm{SU}(2)_W \otimes \mathrm{U}(1)_Y \otimes \mathrm{U}(1)_\chi$, such that the covariant derivative is $D_\mu = D_\mu^{\mathrm{SM}} + iQ'g_\chi Z'_\mu$ with Q' being the dark $\mathrm{U}(1)_\chi$ charge of the relevant fields. We introduce new fields: a Majorana fermion DM candidate χ, a spin-1 dark gauge boson Z', and the dark Higgs field S. We have chosen χ to be Majorana, as a well-motivated example that must involve axial-vector couplings to the Z', given that vector

couplings of Majorana particles vanish. The significance of axial-vector couplings is that perturbative unitarity would be violated at high energy in the absence of S [21]. The dark Higgs is mandatory in this set-up.

The vacuum expectation value (vev) of the dark Higgs field provides a mass generation mechanism for the dark sector fields Z' and χ. For the χ-S Yukawa terms to respect the $\mathrm{U}(1)_\chi$ gauge symmetry, the charge assignments[3] can be chosen, without loss of generality, to be $Q'(S) = 1$ and $Q'(\chi) = -\frac{1}{2}$. The dark Higgs can mix with the SM Higgs H through mass mixing, with strength parameterized by λ_{hs}, while the $\mathrm{U}(1)_\chi$ field strength tensor $Z'_{\mu\nu}$ kinetically mixes with the SM hypercharge field strength $B_{\mu\nu}$ controlled by the kinematic mixing parameter ϵ. Explicitly, before electroweak and dark symmetry breaking, the Lagrangian is written as

$$\begin{aligned}\mathcal{L} = \mathcal{L}_{\mathrm{SM}} + \frac{i}{2}\overline{\chi}\not{\partial}\chi - \frac{1}{4}g_\chi Z'^{\mu}\overline{\chi}\gamma_5\gamma_\mu\chi - \frac{1}{2}y_\chi\overline{\chi}\left(P_L S + P_R S^*\right)\chi \; - \frac{\sin\epsilon}{2}Z'^{\mu\nu}B_{\mu\nu} \\ + \left[(\partial^\mu + ig_\chi Z'^{\mu})S\right]^\dagger\left[(\partial_\mu + ig_\chi Z'_\mu)S\right] - \mu_s^2 S^\dagger S - \lambda_s(S^\dagger S)^2 - \lambda_{hs}(S^\dagger S)(H^\dagger H).\end{aligned} \tag{2.1}$$

After symmetry breaking and mixing the terms of interest are

$$\begin{aligned}\mathcal{L} \supset \frac{1}{2}m_{Z'}^2 Z'^{\mu}Z'_\mu - \frac{1}{2}m_s^2 s^2 - \frac{1}{2}m_\chi\overline{\chi}\chi - \frac{1}{4}g_\chi Z'^{\mu}\overline{\chi}\gamma_5\gamma_\mu\chi - \frac{y_\chi}{2\sqrt{2}}s\overline{\chi}\chi \\ + g_\chi^2 w Z'^{\mu}Z'_\mu s - \lambda_s w s^3 - 2\lambda_{hs}(hvs^2 + swh^2) + g_f\sum_f Z'^{\mu}\overline{f}\Gamma_\mu f,\end{aligned} \tag{2.2}$$

where the component fields of S and H are defined in the broken phase as $S \equiv \frac{1}{\sqrt{2}}(w+s+ia)$ and $H = \left\{G^+, \frac{1}{\sqrt{2}}(v+h+iG^0)\right\}$ with G^+, G^0 and a being the Goldstone bosons of W, Z and Z' respectively, while s and h are real scalars. In the limit that the mixing parameter λ_{hs} is small, the vev of the dark Higgs satisfies $w^2 = -\mu_s^2/\lambda_s$. After symmetry breaking, the masses are

$$m_{Z'} = g_\chi w, \tag{2.3a}$$

$$m_\chi = \frac{1}{\sqrt{2}}y_\chi w, \tag{2.3b}$$

$$m_s^2 \simeq -\mu_s^2, \tag{2.3c}$$

$$m_h \simeq -\mu_h^2. \tag{2.3d}$$

For all couplings to remain perturbative, only certain combinations of the dark gauge coupling and dark sector masses are allowed. From the above equations, the relation between the dark yukawa coupling y_χ and the $\mathrm{U}(1)_\chi$ gauge coupling g_χ is

$$\frac{y_\chi}{g_\chi} = \frac{\sqrt{2}\,m_\chi}{m_{Z'}}. \tag{2.4}$$

[3] In order to cancel anomalies, additional fermions with $\mathrm{U}(1)_\chi$ charge will be required. However, these states can be made sufficiently heavy that they do not affect by the dark sector phenonenology discussed here. For example, anomaly cancellation can be achieved by introducing an additional Majorana fermion, with $\mathrm{U}(1)_\chi$ charge equal in magnitude but of opposite sign to that of χ. It is sufficient to consider only the lighter of the two fermions as the DM candidate, with the heavier making a subdominant contribution to the relic density [57].

JCAP08(2016)001

The final term of eq. (2.2) describes the coupling of Z' to the SM fermions; its structure is dictated by the kinetic mixing, and the explicit form can be found, for example, in ref. [59]. As Z' decays to the SM through the hypercharge portal, the Z' couples to the same SM fields as the SM Z, and no flavor specific tuning is permitted. This enforces strong di-lepton resonance bounds and EWPT limits on Z-Z' mixing. Regardless, the small values of ϵ we consider allow these bounds to be easily satisfied.

Within this model, there are two possible routes for dark sector interactions with the visible sector: the Higgs portal controlled by parameter λ_{hs}, or the hypercharge portal controlled by parameter ϵ. To demonstrate the new phenomenology of the combination of both the Z' and dark Higgs in this model, we will take small values of these parameters consistent with the hidden model setup, and assume both s and Z' decay on-shell to SM fermions. As the Higgs couples to fields proportional to their masses, the dark Higgs decays predominantly to b-quarks in the mass range we consider, although we will fully simulate all final states. The dark Higgs may also decay into two Z' which then may decay into SM fermions, however for simplicity when setting limits we will focus on the region of parameter space where this is not kinematically allowed.

We emphasize that this is the most general scenario involving the interaction of a Majorana fermion with a Z' gauge boson. Given that vector currents vanish for Majorana fermions, leaving only axial-vector interactions, the inclusion of the dark Higgs is unavoidable in order to provide a mass for the Z' within a gauge invariant model that respects perturbative unitarity. Furthermore, it is not possible to include a Majorana mass term for the χ without breaking the $\mathrm{U}(1)_\chi$ symmetry. The case of Dirac dark matter with vector couplings to a Z' would be very different. In that case, the Z' may obtain mass via the Stueckelberg mechanism, and a bare mass term for χ is possible, leaving no need for a dark Higgs.

3 Dark matter annihilation processes for indirect detection

In this section we will calculate the annihilation cross sections and branching fractions relevant for indirect detection.

3.1 Annihilation cross sections

The novel process for DM annihilation in the universe today is $\chi\chi \to sZ'$, which is shown in figure 3. This process has not been considered in previous work, despite being a consequence of a self-consistent Z' model with axial-vector couplings. The cross section for $\chi\chi \to sZ'$ is s-wave for both scalar and pseudoscalar interactions, and vector or axial-vector Z'-DM couplings. For Majorana DM and a real scalar the annihilation cross section is given by

$$\langle \sigma v \rangle_{\chi\chi \to sZ'} = \frac{g_\chi^4 \left(m_s^4 - 2m_s^2 \left(m_{Z'}^2 + 4m_\chi^2 \right) + \left(m_{Z'}^2 - 4m_\chi^2 \right)^2 \right)^{3/2}}{1024\pi m_\chi^4 m_{Z'}^4}, \tag{3.1}$$

where eq. (2.4) has been used to replace y_χ. Here, only the s-channel diagram of figure 3 contributes an s-wave component.

JCAP08(2016)001

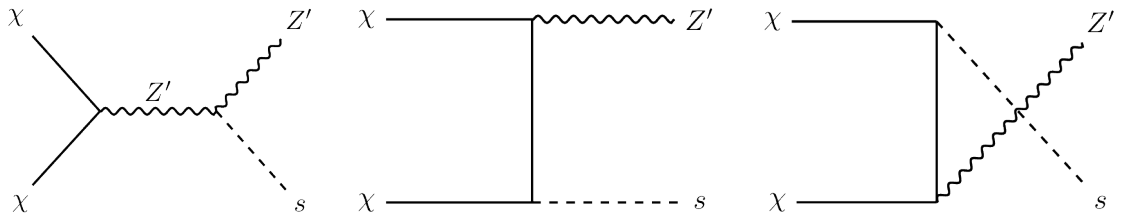

Figure 3. Annihilation diagrams for the s-wave processes $\chi\chi \to sZ'$. The scalar and the Z' then can decay to SM fermion final states. For some regions of parameter space this is the only kinematically allowed process, while in others it can have a cross section larger than the process in figure 4. This process can be achieved by considering the simplified model benchmarks together.

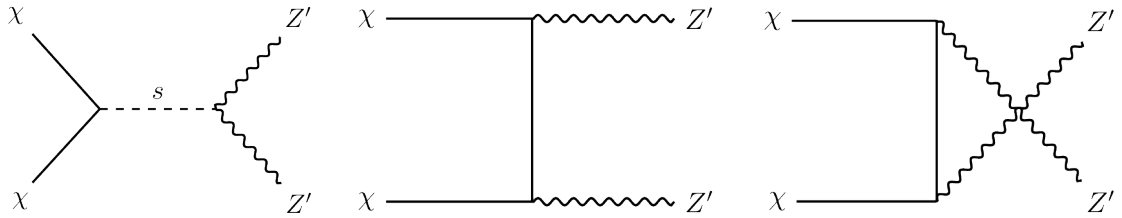

Figure 4. Annihilation diagrams for the s-wave processes $\chi\chi \to Z'Z'$. The Z' then can decay into SM fermion final states. In the spin-1 mediator simplified model benchmark, only the t-channel and u-channel diagrams appear, leading to unitarity issues at high energies for axial couplings. In our gauge invariant model, the s-channel diagram restores perturbative unitarity. Consideration of only $\chi\chi \to Z'Z'$, without the accompanying $\chi\chi \to sZ'$ process of figure 3 will lead to inaccurate conclusions.

The other dominant s-wave process in this model is $\chi\chi \to Z'Z'$, which is shown in figure 4. For Majorana DM, the s-wave contribution to its cross section is given by[4]

$$\langle \sigma v \rangle_{\chi\chi \to Z'Z'} = \frac{g_\chi^4 \left(1 - \frac{m_{Z'}^2}{m_\chi^2}\right)^{3/2}}{256\pi m_\chi^2 \left(1 - \frac{m_{Z'}^2}{2m_\chi^2}\right)^2}\,, \tag{3.2}$$

where the s-wave contributions only come from the t and u channel diagrams, making the indirect signal for the $Z'Z'$ process the same as that found in the spin-1 simplified model benchmark.

Previously, annihilation of fermionic dark matter to spin-0 mediators featured an s-wave component only for the three-body phase-space suppressed process in figure 2, and only for pseudoscalars. For a simplified model with a scalar mediator, there is no s-wave annihilation process at all. We make the important observation that annihilation of fermionic dark matter to a spin-0 plus spin-1 final state will always be s-wave, for both scalars and pseudoscalars. This allows indirect detection to have comparable sensitivity for spin-0 and spin-1 mediators, in models where the two mediators are both present. This is realized naturally in the very simple gauge invariant model we have presented in this paper.

[4]The factor of 16 difference between our cross section and that given in other papers is due to the $(Q'_\chi)^4 = (1/2)^4$ charge contribution to the coefficient.

JCAP08(2016)001

As this new s-wave annihilation process is a consequence of enforcing perturbative unitarity at high energies, its presence is inevitable for axial-vector Z'-DM couplings. This means that the limits on indirect detection signals using the $Z'Z'$ process alone will lead to inaccurate conclusions. This can be seen in figure 5, where we plot the annihilation cross sections to both the $Z'Z'$ and sZ' final states. If the s is lighter than the Z', there are values of DM mass $m_s + m_{Z'} < 2m_\chi < 2m_{Z'}$ where sZ' is the only kinematically accessible final state. If we were to only consider the $Z'Z'$ process, it would not be possible to produce a limit for these low DM masses (where, in fact, the indirect detection limits are the strongest). When both sZ' and $Z'Z'$ are kinematically accessible, sZ' becomes the dominant process. In the limit $m_\chi^2 \gg m_{Z'}^2, m_s^2$, the cross section to sZ' is enhanced relative to that for $Z'Z'$ by a factor of $(m_\chi/m_{Z'})^4$, arising due to the longitudinal Z' polarization. It is important to note, however, that the DM mass and Z' mass are related via the dark Higgs vev, and thus satisfy eq. (2.4). As a result, it is not possible to make the DM mass arbitrarily large while retaining a perturbative value for the Yukawa coupling y_χ. For the mass ranges plotted in figure 5, we have ensured that all parameters take reasonable values.

The s-wave annihilations to sZ' and $Z'Z'$ are by far the dominant processes for indirect detection, for which the total annihilation cross section is obtained by summing the contributions from these channels. In setting indirect detection limits, the energy spectra should be computed by properly combining the spectra arising from the sZ' and $Z'Z'$ final states. These s-wave processes will also be the most important for the determination of relic density at freezeout. However, p-wave processes will also play a role at freezeout, where the DM relative velocity is much larger than in the universe today. Note that as the cross sections in figure 5 each scale as g_χ^4, the correct thermal relic density can easily be obtained simply by adjusting the value of the dark gauge coupling.

3.2 Decay widths of the dark Higgs and Z'

To compare our annihilation processes to indirect detection signals, it is necessary to first multiply the thermal averaged cross sections for our on-shell processes by relevant branching fractions. The Z' decays to SM states via the hypercharge portal, and so couplings to all fermion flavors must be considered. The partial decay width of the Z' into SM fermions is given by

$$\Gamma(Z' \to f\bar{f}) = \frac{m_{Z'} N_c}{12\pi} \sqrt{1 - \frac{4m_f^2}{m_{Z'}^2}} \left[g_{f,V}^2 \left(1 + \frac{2m_f^2}{m_{Z'}^2}\right) + g_{f,A}^2 \left(1 - \frac{4m_f^2}{m_{Z'}^2}\right) \right], \tag{3.3}$$

where N_c is a color factor, relevant for hadronic decays. The $g_{f,V}$ (vector) and $g_{f,A}$ (axial-vector) coupling structures of the Z' to the SM are inherited from the kinetic mixing with the SM. The total decay width for the Z' is simply the sum of all the fermionic decays,

$$\Gamma'_Z = \sum_f \Gamma(Z' \to f\bar{f}). \tag{3.4}$$

The dark Higgs decays to the SM due to mass mixing with the SM Higgs. As it couples to fermions through their mass, the decay will be predominantly to b quarks in the mass ranges we are considering, however we include all SM final states for accuracy. The dark Higgs is also permitted to decay to pairs of Z', although for simplicity we will choose parameters where this decay is not kinematically permitted. As loop decays and higher order corrections can be relevant for the dark Higgs decays, to ensure an accurate calculation of the branching fractions, we use the FORTRAN package HDECAY [60], which takes these effects into account.

JCAP08(2016)001

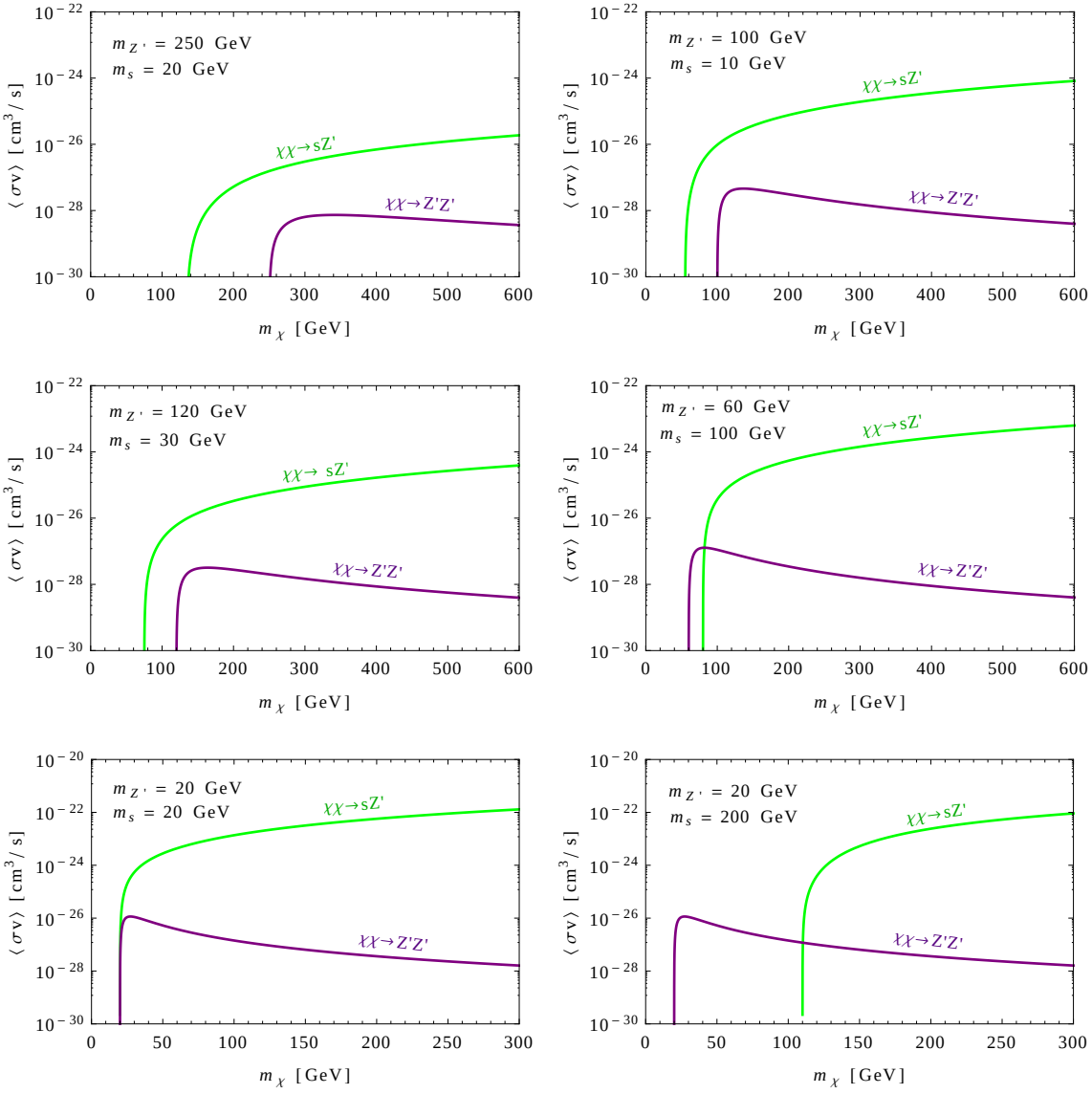

Figure 5. Relative cross section sizes for the two dominant s-wave diagrams, $\chi\chi \to sZ'$ (green) and $\chi\chi \to Z'Z'$ (purple), for some example parameter choices for the dark Higgs mass m_s and the Z' mass $m_{Z'}$, as labelled on each plot. For all plots the gauge coupling is set to $g_\chi = 0.1$, but as all cross sections are directly proportional to g_χ^4 they can easily be scaled by adjusting this parameter. Note the lower two plots have a different m_χ range to the upper plots, so that the y_χ coupling is restricted to $\mathcal{O}(1)$ values.

4 γ-ray energy spectra

The gamma ray flux Φ from photons with energy E_γ resulting from dark matter annihilation into a fermion species f is

$$\frac{d^2\Phi}{d\Omega dE_\gamma} = \frac{\langle\sigma v\rangle}{8\pi m_\chi^2}\left(\sum_f \frac{dN}{dE_\gamma} Br_f\right) J(\phi,\gamma), \tag{4.1}$$

JCAP08(2016)001

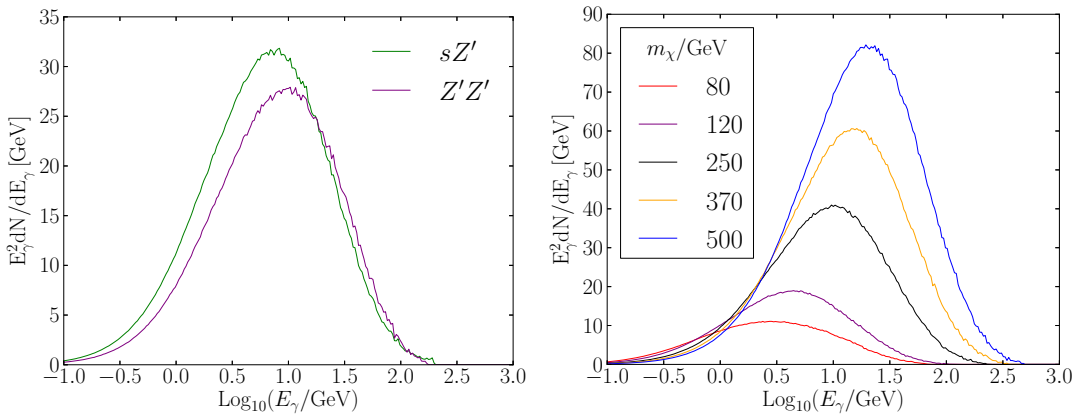

Figure 6. Left: comparison of gamma ray spectra for DM annihilation into sZ' vs. $Z'Z'$ for example parameters $m_s = 100\,\mathrm{GeV}$, $m_{Z'} = 60\,\mathrm{GeV}$ and $m_\chi = 200\,\mathrm{GeV}$. Right: Gamma ray spectra for DM annihilation to sZ' with $m_s = 30\,\mathrm{GeV}$ and $m_{Z'} = 120\,\mathrm{GeV}$, for various DM masses. These plots include decays to all SM final states.

where Br_f is the branching fraction to the particular fermion species. For the Z' we take this as the ratio of eq. (3.3) and eq. (3.4). For the dark Higgs, we generate values using HDecay [60]. The J factor is the integral over the line of sight of the DM density $\rho(r)$ squared, at a distance r from the center of the galaxy [61],

$$J(\phi, \gamma) = \int \rho^2(r) dl, \tag{4.2}$$

where the DM density is taken to be modelled by the Navarro-Frenk-White (NFW) profile. The numerical values of the J-factors and their uncertainties together with other properties of the dSphs are listed in table I of ref. [62].

To obtain our γ-ray spectra, we simulate the annihilation cascade for a given DM mass with an effective resonance in Pythia [63]. In our setup, it is possible to have two different on-shell states which decay to SM fermions: the Z' and the dark Higgs. To model for our different states, we produce one diagram with two Z' and one with two dark Higgs, both with effective resonances in their center of mass frames. We then average these to produce the effective spectra for a given DM mass. Specifically, the effective resonances for different Z' and dark Higgs s masses are respectively given by [59]

$$E^{Z'}_{CoM} = \frac{s + m^2_{Z'} - m^2_s}{2\sqrt{s}}, \quad E^{s}_{CoM} = \frac{s + m^2_s - m^2_{Z'}}{2\sqrt{s}}. \tag{4.3}$$

Example gamma ray spectra including all possible fermionic SM final states are shown in figure 6, as well as a comparison of the sZ' and $Z'Z'$ spectra for example parameters.

5 Annihilation limits from dwarf spheriodal galaxies and AMS-02

Currently, two of the strongest constraints on dark matter annihilation processes come from AMS-02, for low DM masses and electron-positron final states, and from Fermi-LAT limits placed on signals from dwarf spheriodal satellite galaxies of the Milky Way [62]. Dwarf spheriodal galaxies (dSphs) are particularly useful in constraining dark matter models, as according to kinematic data they are one of the most dark matter dense objects in the sky,

JCAP08(2016)001

and have relatively low backgrounds. However, the limits published by Fermi-LAT assume a 100% branching fraction to a particular SM final state, and within our kinetically mixed Z' model this will not be true due to the flavor universal nature of the mixing. It is also not trivial to simply scale the dSphs limits with our branching fractions, as not only are the kinematics are different, but as there can be cross-polution of photon contributions from different final states. Furthermore, our new process $\chi\chi \to sZ'$ has two different final state particles with different masses, and the resulting spectra will depend on the specific masses of these particles. Therefore it is necessary to recast the limits for this specific setup, comparing to the dSphs likelihood functions released by Fermi-LAT.

To find the limit on the cross section from dSphs, we use our spectra generated with Pythia [63], as described in the previous section. We then use the maximal likelihood method to compare our spectra against those for the dSphs publically provided by Fermi-LAT in the Pass 8 data, with the J factor taken to be a nuisance parameter as per ref. [62]. The Pass 8 data is six years of LAT data taken from 2008-08-04 to 2014-08-05 and further selected with Pass 8 SOURCE-class in the energy range between 500 MeV and 500 GeV. We take spectra from 15 dSphs: Bootes I, Canes Venatici II, Carina, Coma Berenices, Draco, Fornax, Hercules, Leo II, Leo IV, Sculptor, Segue 1, Sextans, Ursa Major II, Ursa Minor, and Willman 1. The 95% C.L. limits on the annihilation cross section from dSphs for both $Z'Z'$ and sZ' spectra are shown for some example parameters in figure 7.

In figure 7, limits are set on the individual sZ' and $Z'Z'$ cross sections, where the benchmark parameters demonstrate the variation between expected results for different masses; we show examples where $m_s = m_{Z'}$, $m_s > m_{Z'}$ and $m_s < m_{Z'}$. In general, the limits arising from the spectral shape of the DM annihilation to sZ' is slightly more constraining than that from $Z'Z'$. This is likely due to the peak of the gamma ray spectra produced by the scalar being higher than that produced by the Z'. Which limit is relevant depends on which of the final states is kinematically accessible. When sZ' is accessible it greatly dominates, and hence the cross section limit is given by the solid green sZ' line. If $Z'Z'$ but not sZ' is accessible then the solid purple $Z'Z'$ line shows the relevant limit, which is shown for the lower mass region in the benchmark for $m_s > m_{Z'}$: $m_s = 100\,\text{GeV}$ and $m_{Z'} = 60\,\text{GeV}$. All other mass choices will resemble these examples, depending on the hierarchy of the masses of the Z' and the dark Higgs. The heavier (lighter) the masses are, the weaker (stronger) the cross section limit will be. However, it is clear when comparing the cases of $m_{Z'} = 20\,\text{GeV}$ and 250 GeV (figure 7 top left and bottom right), the difference in the limit is minimal, apart from the fact that the limit will begin at higher DM masses for the processes to be kinematically accessible. The purple dotted line corresponds to the limit on annihilation to $Z'Z'$ alone, as would occur in a simplified model with only a Z' mediator and no dark Higgs. This allows for a comparision of the simplified model with our scenario.

To find the limit from AMS-02, it is sufficient to only consider electron-positron final states, as these provide the strongest limits. As the dark Higgs couples to particles through their mass, there will be negligible production of electron final states via decay of the s. This means that the Z' decays will provide effectively all the electron-positron signal. In the low DM mass range, where AMS-02 is most constraining, the limit on the cross section is approximately flat for cascade decays to two identical final state particles [34]. Therefore, we scale the cross section limit on electron final states by the branching fraction of Z' to electron-positron pairs. This is stronger than the dSphs limit only for low DM masses (and hence low s and Z' masses). As a result, AMS-02 limits are relevant only for low mass parameters, and shown on only one of the plots of figure 7 for which the Z' and s masses are both small.

JCAP08(2016)001

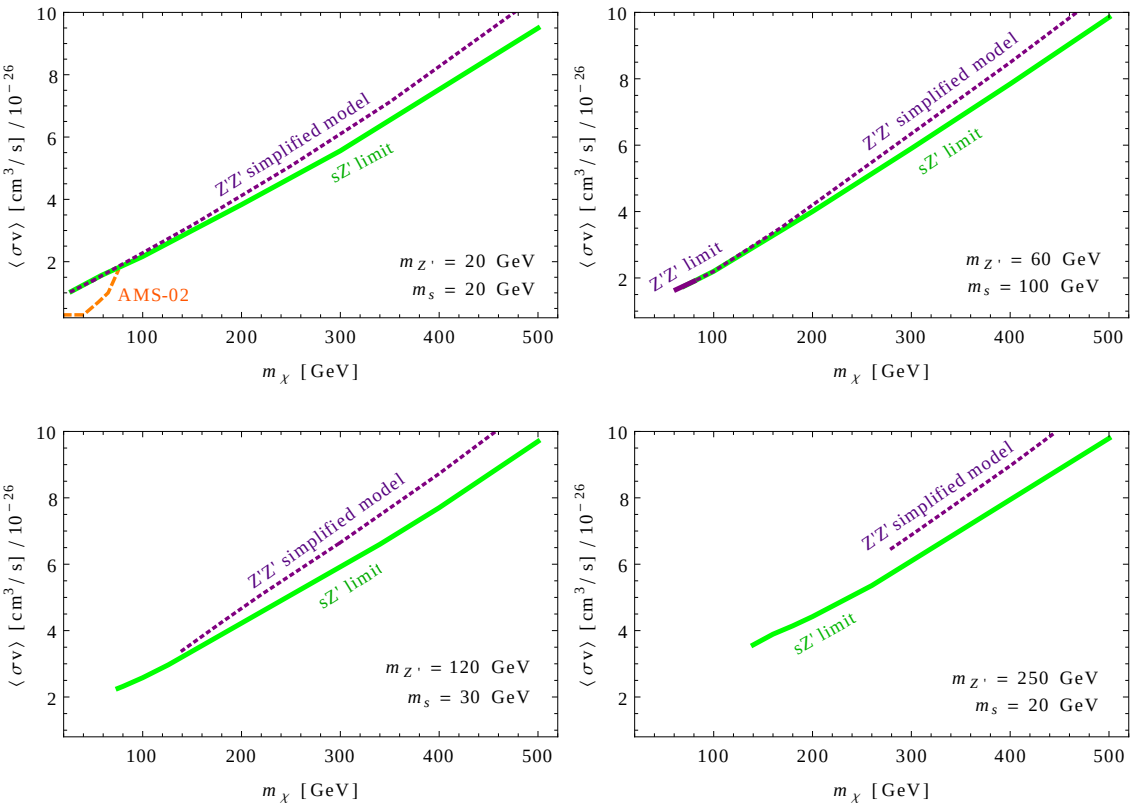

Figure 7. 95% confidence limits (C.L.) on the annihilation cross section from Fermi data on 15 dwarf spheroidal galaxies. All solid lines are limits on our model: the purple line is the cross section limit arising from the $Z'Z'$ process is alone; the green line is the cross section limit for the sZ' process alone. The purple dotted line is the $Z'Z'$ limit alone as per the simplified model with no dark Higgs. The approximate limit from AMS-02 is shown in orange. Masses are as labelled in each plot.

6 Other model constraints

The indirect detection constraints are determined purely by the couplings of the mediators to DM, controlled by g_χ, and the mass parameters m_χ, $m_{Z'}$ and m_s. The exact size of the small couplings of the mediators to SM fermions, controlled by the mixing parameters ϵ and λ_{hs}, does not affect the indirect detection signals, as the mediators have long astrophysical time scales over which to eventually decay. However, other experimental probes, such as direct detection and collider experiments, are directly sensitive to the size of the small dark-SM couplings.

6.1 Collider and direct detection constraints

As the couplings between the dark and visible sectors are taken to be very small, it is possible to completely escape the strong WIMP DM constraints from the LHC and direct detection. This provides a compelling scenario which is consistent with the null results of these experiements to date, while still allowing a large indirect detecion signal.

JCAP08(2016)001

6.2 BBN and CMB constraints

A lower limit on the size of the couplings between the sectors comes from Big Bang Nucleosynthesis (BBN), which requires that the mediators have a lifetime of $\tau < 1$s [64]. This leaves a large range of values (several orders of magnitude) for the kinematic mixing parameter ϵ and Higgs portal parameter λ_{hs}. In addition, CMB measurements can also provide constraints on the annihilation cross sections, however they are weaker than those arising from AMS-02 and dSphs [34].

6.3 Unitarity

As discussed above, the dark Higgs is included not only to provide a mass generation mechanism for the dark sector, but to ensure perturbative unitarity is not violated at high energies. In the absence of the scalar, unitarity violation would arise at high energy due to the longitudinal mode of the Z' gauge boson in processes such as $\chi\chi \to Z'Z'$.

In the indirect detection context, where it is appropriate to take the zero velocity limit, it turns out that the cross section for $\chi\chi \to Z'Z'$ receives no contribution from the scalar exchange diagram of figure 4. However, at high energies where the $v = 0$ threshold approximation is no longer valid (including at freezeout) the scalar diagram cannot be neglected [57]. Regardless, the scalar is mandatory in any model in which the Z' has axial-vector couplings to fermions, in order to properly respect gauge invariance and perturbative unitarity [21].

7 Summary

We have considered a self-consistent dark sector containing a Majorana fermion DM candidate, χ, a dark gauge boson, Z', and a dark Higgs, s, which transform under a dark $\mathrm{U}(1)_\chi$ gauge symmetry. This is the minimal consistent model in which a Majorana DM candidate couples to a spin-1 mediator. In this scenario, the coupling of the DM to the Z' must be of axial-vector form, as vector couplings of Majorana fermions vanish. The dark Higgs field provides a mass generation mechanism for both the Z' gauge boson and the DM χ, and is required in order for the model to properly respect gauge invariance and perturbative unitarity.

We have investigated the indirect detection phenomenology of this model, focusing on the processes where the DM annihilates to on-shell dark sector mediators. We found that the presence of a spin-0 and spin-1 mediator in the same model opens up an important new s-wave annihilation channel, $\chi\chi \to sZ'$, which can dominate over the well-studied process $\chi\chi \to Z'Z'$. This is to be contrasted to the situtation in simplified models that contain a single mediator: there is no s-wave annihilation process to scalar mediators; s-wave annihilation to pseudoscalar mediators is suppressed by 3-body phase space; the process $\chi\chi \to Z'Z'$ is the only s-wave annihilation to vector or axial-vector mediators (which, in the case of an axial mediator, violates unitarity at high energy). The inclusion of the scalar and vector mediator in the same model allows sizable production of the scalar mediator via s-wave annihilation, which was previously not thought possible, and provides a very plausible way to discover the dark Higgs. This important phenomenology is missed in the single-mediator simplified model approach.

We have calculated indirect detection limits on the sZ' and $Z'Z'$ annihilation processes, using Fermi-LAT gamma ray data for dwarf spheriodal galaxies. The gamma ray energy spectra resulting from the two annihilation modes are similar. Depending on the masses of the dark sector particles, there are regions of parameter space where only one of the sZ'

JCAP08(2016)001

and $Z'Z'$ final states are kinematically accessible. As such, the new process allows a broader range of DM masses to be probed via indirect detection. In the limit that $m_\chi^2 \gg m_{Z'}^2, m_s^2$, where both processes are kinematically allowed, the cross sections to sZ' is much greater than that to $Z'Z'$. Neglecting the sZ' process, as done in the simplified model setup, would lead to highly inaccurate constraints on the model parameters.

An important observation is that the mass and coupling parameters in the dark sector may be intrinsically related to each other. In our case, the various parameters are related via the gauge coupling constant and the dark Higgs vev, such that we do not have the freedom to vary all parameters independently. The absence of this feature is one of the shortcomings of the (albeit very useful) simplified model approach. In general, renormalizable models in which gauge invariance is enforced will be a superior approach. Not only are unitarity problems avoided, but the phenomenology is potentially richer.

Acknowledgments

This work was supported in part by the Australian Research Council. Feynman diagrams are drawn using TikZ-Feynman [65]. We thank the authors of ref. [29] for pointing out an error in an earlier version of our cross section.

References

[1] L. Bergström, *Nonbaryonic dark matter: Observational evidence and detection methods*, *Rept. Prog. Phys.* **63** (2000) 793 [hep-ph/0002126] [INSPIRE].

[2] G. Bertone, D. Hooper and J. Silk, *Particle dark matter: Evidence, candidates and constraints*, *Phys. Rept.* **405** (2005) 279 [hep-ph/0404175] [INSPIRE].

[3] J. Abdallah et al., *Simplified Models for Dark Matter and Missing Energy Searches at the LHC*, arXiv:1409.2893 [INSPIRE].

[4] M.R. Buckley, D. Feld and D. Goncalves, *Scalar Simplified Models for Dark Matter*, *Phys. Rev.* **D 91** (2015) 015017 [arXiv:1410.6497] [INSPIRE].

[5] LHC New Physics Working Group collaboration, D. Alves et al., *Simplified Models for LHC New Physics Searches*, *J. Phys.* **G 39** (2012) 105005 [arXiv:1105.2838] [INSPIRE].

[6] J. Alwall, P. Schuster and N. Toro, *Simplified Models for a First Characterization of New Physics at the LHC*, *Phys. Rev.* **D 79** (2009) 075020 [arXiv:0810.3921] [INSPIRE].

[7] J. Abdallah et al., *Simplified Models for Dark Matter Searches at the LHC*, *Phys. Dark Univ.* **9-10** (2015) 8 [arXiv:1506.03116] [INSPIRE].

[8] D. Abercrombie et al., *Dark Matter Benchmark Models for Early LHC Run-2 Searches: Report of the ATLAS/CMS Dark Matter Forum*, arXiv:1507.00966 [INSPIRE].

[9] A. De Simone and T. Jacques, *Simplified Models vs. Effective Field Theory Approaches in Dark Matter Searches*, *Eur. Phys. J.* **C 76** (2016) 367 [arXiv:1603.08002] [INSPIRE].

[10] T. Jacques, A. Katz, E. Morgante, D. Racco, M. Rameez and A. Riotto, *Complementarity of DM Searches in a Consistent Simplified Model: the Case of Z'*, arXiv:1605.06513 [INSPIRE].

[11] I.M. Shoemaker and L. Vecchi, *Unitarity and Monojet Bounds on Models for DAMA, CoGeNT and CRESST-II*, *Phys. Rev.* **D 86** (2012) 015023 [arXiv:1112.5457] [INSPIRE].

[12] P.J. Fox, R. Harnik, R. Primulando and C.-T. Yu, *Taking a Razor to Dark Matter Parameter Space at the LHC*, *Phys. Rev.* **D 86** (2012) 015010 [arXiv:1203.1662] [INSPIRE].

JCAP08(2016)001

[13] G. Busoni, A. De Simone, E. Morgante and A. Riotto, *On the Validity of the Effective Field Theory for Dark Matter Searches at the LHC*, *Phys. Lett.* **B 728** (2014) 412 [arXiv:1307.2253] [INSPIRE].

[14] O. Buchmueller, M.J. Dolan and C. McCabe, *Beyond Effective Field Theory for Dark Matter Searches at the LHC*, *JHEP* **01** (2014) 025 [arXiv:1308.6799] [INSPIRE].

[15] G. Busoni, A. De Simone, J. Gramling, E. Morgante and A. Riotto, *On the Validity of the Effective Field Theory for Dark Matter Searches at the LHC, Part II: Complete Analysis for the s-channel*, *JCAP* **06** (2014) 060 [arXiv:1402.1275] [INSPIRE].

[16] M. Endo and Y. Yamamoto, *Unitarity Bounds on Dark Matter Effective Interactions at LHC*, *JHEP* **06** (2014) 126 [arXiv:1403.6610] [INSPIRE].

[17] G. Busoni, A. De Simone, T. Jacques, E. Morgante and A. Riotto, *On the Validity of the Effective Field Theory for Dark Matter Searches at the LHC Part III: Analysis for the t-channel*, *JCAP* **09** (2014) 022 [arXiv:1405.3101] [INSPIRE].

[18] S. El Hedri, W. Shepherd and D.G.E. Walker, *Perturbative Unitarity Constraints on Gauge Portals*, arXiv:1412.5660 [INSPIRE].

[19] N.F. Bell, Y. Cai, J.B. Dent, R.K. Leane and T.J. Weiler, *Dark matter at the LHC: Effective field theories and gauge invariance*, *Phys. Rev.* **D 92** (2015) 053008 [arXiv:1503.07874] [INSPIRE].

[20] S. Baek, P. Ko, M. Park, W.-I. Park and C. Yu, *Beyond the Dark matter effective field theory and a simplified model approach at colliders*, *Phys. Lett.* **B 756** (2016) 289 [arXiv:1506.06556] [INSPIRE].

[21] F. Kahlhoefer, K. Schmidt-Hoberg, T. Schwetz and S. Vogl, *Implications of unitarity and gauge invariance for simplified dark matter models*, *JHEP* **02** (2016) 016 [arXiv:1510.02110] [INSPIRE].

[22] N.F. Bell, Y. Cai and R.K. Leane, *Mono-W Dark Matter Signals at the LHC: Simplified Model Analysis*, *JCAP* **01** (2016) 051 [arXiv:1512.00476] [INSPIRE].

[23] U. Haisch, F. Kahlhoefer and T.M.P. Tait, *On Mono-W Signatures in Spin-1 Simplified Models*, *Phys. Lett.* **B 760** (2016) 207 [arXiv:1603.01267] [INSPIRE].

[24] C. Englert, M. McCullough and M. Spannowsky, *S-Channel Dark Matter Simplified Models and Unitarity*, arXiv:1604.07975 [INSPIRE].

[25] N. Bell, G. Busoni, A. Kobakhidze, D.M. Long and M.A. Schmidt, *Unitarisation of EFT Amplitudes for Dark Matter Searches at the LHC*, arXiv:1606.02722 [INSPIRE].

[26] J.M. Cline, G. Dupuis, Z. Liu and W. Xue, *Multimediator models for the galactic center gamma ray excess*, *Phys. Rev.* **D 91** (2015) 115010 [arXiv:1503.08213] [INSPIRE].

[27] A. Choudhury, K. Kowalska, L. Roszkowski, E.M. Sessolo and A.J. Williams, *Less-simplified models of dark matter for direct detection and the LHC*, *JHEP* **04** (2016) 182 [arXiv:1509.05771] [INSPIRE].

[28] K. Ghorbani and H. Ghorbani, *Two-portal Dark Matter*, *Phys. Rev.* **D 91** (2015) 123541 [arXiv:1504.03610] [INSPIRE].

[29] M. Duerr, F. Kahlhoefer, K. Schmidt-Hoberg, T. Schwetz and S. Vogl, *How to save the WIMP: global analysis of a dark matter model with two s-channel mediators*, arXiv:1606.07609 [INSPIRE].

[30] A. Martin, J. Shelton and J. Unwin, *Fitting the Galactic Center Gamma-Ray Excess with Cascade Annihilations*, *Phys. Rev.* **D 90** (2014) 103513 [arXiv:1405.0272] [INSPIRE].

JCAP08(2016)001

[31] M. Abdullah, A. DiFranzo, A. Rajaraman, T.M.P. Tait, P. Tanedo and A.M. Wijangco, *Hidden on-shell mediators for the Galactic Center γ-ray excess*, *Phys. Rev.* **D 90** (2014) 035004 [arXiv:1404.6528] [INSPIRE].

[32] A. Berlin, P. Gratia, D. Hooper and S.D. McDermott, *Hidden Sector Dark Matter Models for the Galactic Center Gamma-Ray Excess*, *Phys. Rev.* **D 90** (2014) 015032 [arXiv:1405.5204] [INSPIRE].

[33] G. Elor, N.L. Rodd and T.R. Slatyer, *Multistep cascade annihilations of dark matter and the Galactic Center excess*, *Phys. Rev.* **D 91** (2015) 103531 [arXiv:1503.01773] [INSPIRE].

[34] G. Elor, N.L. Rodd, T.R. Slatyer and W. Xue, *Model-Independent Indirect Detection Constraints on Hidden Sector Dark Matter*, *JCAP* **06** (2016) 024 [arXiv:1511.08787] [INSPIRE].

[35] W. Chao, M.J. Ramsey-Musolf and J.-H. Yu, *Indirect Detection Imprint of a CP-violating Dark Sector*, *Phys. Rev.* **D 93** (2016) 095025 [arXiv:1602.05192] [INSPIRE].

[36] M. Pospelov, A. Ritz and M.B. Voloshin, *Secluded WIMP Dark Matter*, *Phys. Lett.* **B 662** (2008) 53 [arXiv:0711.4866] [INSPIRE].

[37] M. Pospelov and A. Ritz, *Astrophysical Signatures of Secluded Dark Matter*, *Phys. Lett.* **B 671** (2009) 391 [arXiv:0810.1502] [INSPIRE].

[38] M. Pospelov, *Secluded* U(1) *below the weak scale*, *Phys. Rev.* **D 80** (2009) 095002 [arXiv:0811.1030] [INSPIRE].

[39] J.L. Feng, H. Tu and H.-B. Yu, *Thermal Relics in Hidden Sectors*, *JCAP* **10** (2008) 043 [arXiv:0808.2318] [INSPIRE].

[40] J.L. Feng and J. Kumar, *The WIMPless Miracle: Dark-Matter Particles without Weak-Scale Masses or Weak Interactions*, *Phys. Rev. Lett.* **101** (2008) 231301 [arXiv:0803.4196] [INSPIRE].

[41] I.Z. Rothstein, T. Schwetz and J. Zupan, *Phenomenology of Dark Matter annihilation into a long-lived intermediate state*, *JCAP* **07** (2009) 018 [arXiv:0903.3116] [INSPIRE].

[42] J. Mardon, Y. Nomura and J. Thaler, *Cosmic Signals from the Hidden Sector*, *Phys. Rev.* **D 80** (2009) 035013 [arXiv:0905.3749] [INSPIRE].

[43] J. Mardon, Y. Nomura, D. Stolarski and J. Thaler, *Dark Matter Signals from Cascade Annihilations*, *JCAP* **05** (2009) 016 [arXiv:0901.2926] [INSPIRE].

[44] P. Meade, M. Papucci and T. Volansky, *Dark Matter Sees The Light*, *JHEP* **12** (2009) 052 [arXiv:0901.2925] [INSPIRE].

[45] C. Cheung, G. Elor, L.J. Hall and P. Kumar, *Origins of Hidden Sector Dark Matter I: Cosmology*, *JHEP* **03** (2011) 042 [arXiv:1010.0022] [INSPIRE].

[46] H. Davoudiasl and I.M. Lewis, *Dark Matter from Hidden Forces*, *Phys. Rev.* **D 89** (2014) 055026 [arXiv:1309.6640] [INSPIRE].

[47] J. Liu, N. Weiner and W. Xue, *Signals of a Light Dark Force in the Galactic Center*, *JHEP* **08** (2015) 050 [arXiv:1412.1485] [INSPIRE].

[48] E. Hardy, R. Lasenby and J. Unwin, *Annihilation Signals from Asymmetric Dark Matter*, *JHEP* **07** (2014) 049 [arXiv:1402.4500] [INSPIRE].

[49] C. Boehm, M.J. Dolan and C. McCabe, *A weighty interpretation of the Galactic Centre excess*, *Phys. Rev.* **D 90** (2014) 023531 [arXiv:1404.4977] [INSPIRE].

[50] S.D. McDermott, *Lining up the Galactic Center Gamma-Ray Excess*, *Phys. Dark Univ.* **7-8** (2015) 12 [arXiv:1406.6408] [INSPIRE].

JCAP08(2016)001

[51] Z. Chacko, Y. Cui, S. Hong and T. Okui, *Hidden dark matter sector, dark radiation and the CMB*, *Phys. Rev.* **D 92** (2015) 055033 [arXiv:1505.04192] [INSPIRE].

[52] P. Ko and Y. Tang, *Dark Higgs Channel for FERMI GeV γ-ray Excess*, *JCAP* **02** (2016) 011 [arXiv:1504.03908] [INSPIRE].

[53] P. Ko, W.-I. Park and Y. Tang, *Higgs portal vector dark matter for* GeV *scale γ-ray excess from galactic center*, *JCAP* **09** (2014) 013 [arXiv:1404.5257] [INSPIRE].

[54] Y.G. Kim, K.Y. Lee, C.B. Park and S. Shin, *Secluded singlet fermionic dark matter driven by the Fermi gamma-ray excess*, *Phys. Rev.* **D 93** (2016) 075023 [arXiv:1601.05089] [INSPIRE].

[55] D. Hooper, N. Weiner and W. Xue, *Dark Forces and Light Dark Matter*, *Phys. Rev.* **D 86** (2012) 056009 [arXiv:1206.2929] [INSPIRE].

[56] A. Berlin, S. Gori, T. Lin and L.-T. Wang, *Pseudoscalar Portal Dark Matter*, *Phys. Rev.* **D 92** (2015) 015005 [arXiv:1502.06000] [INSPIRE].

[57] J.M. Cline, G. Dupuis, Z. Liu and W. Xue, *The windows for kinetically mixed Z'-mediated dark matter and the galactic center gamma ray excess*, *JHEP* **08** (2014) 131 [arXiv:1405.7691] [INSPIRE].

[58] D.E. Morrissey and A.P. Spray, *New Limits on Light Hidden Sectors from Fixed-Target Experiments*, *JHEP* **06** (2014) 083 [arXiv:1402.4817] [INSPIRE].

[59] Particle Data Group collaboration, K.A. Olive et al., *Review of Particle Physics*, *Chin. Phys.* **C 38** (2014) 090001 [INSPIRE].

[60] A. Djouadi, J. Kalinowski and M. Spira, *HDECAY: A Program for Higgs boson decays in the standard model and its supersymmetric extension*, *Comput. Phys. Commun.* **108** (1998) 56 [hep-ph/9704448] [INSPIRE].

[61] M. Cirelli et al., *PPPC 4 DM ID: A Poor Particle Physicist Cookbook for Dark Matter Indirect Detection*, *JCAP* **03** (2011) 051 [*Erratum ibid.* **1210** (2012) E01] [arXiv:1012.4515] [INSPIRE].

[62] Fermi-LAT collaboration, M. Ackermann et al., *Searching for Dark Matter Annihilation from Milky Way Dwarf Spheroidal Galaxies with Six Years of Fermi Large Area Telescope Data*, *Phys. Rev. Lett.* **115** (2015) 231301 [arXiv:1503.02641] [INSPIRE].

[63] T. Sjöstrand et al., *An Introduction to PYTHIA 8.2*, *Comput. Phys. Commun.* **191** (2015) 159 [arXiv:1410.3012] [INSPIRE].

[64] F. Chen, J.M. Cline and A.R. Frey, *Nonabelian dark matter: Models and constraints*, *Phys. Rev.* **D 80** (2009) 083516 [arXiv:0907.4746] [INSPIRE].

[65] J. Ellis, *TikZ-Feynman: Feynman diagrams with TikZ*, arXiv:1601.05437 [INSPIRE].

JCAP08(2016)001